Available online at www.sciencedirect.com
ScienceDirect
Journal of Solid State Chemistry 181 (2008) 567–575
JOURNAL OF SOLID STATE CHEMISTRY
www.elsevier.com/locate/jssc

Syntheses, structures, luminescence, and magnetism of four 3D lanthanide 5-sulfosalicylates

Rui-Sha Zhou, Ling Ye, Hong Ding, Jiang-Feng Song, Xiao-Yu Xu, Ji-Qing Xu*

College of Chemistry and State Key Laboratory of Inorganic Synthesis and Preparative Chemistry, Jilin University, Changchun, Jilin 130021, P.R. China

Received 21 October 2007; received in revised form 24 December 2007; accepted 27 December 2007
Available online 1 January 2008

Abstract

Four 3D lanthanide(III) complexes with 5-sulfosalicylic acid (H_3SSA) as bridging ligands, $Ln(SSA)(H_2O)_2$ [Ln = Ce(III) (**1**), Pr(III) (**2**), Nd(III) (**3**) and Dy(III) (**4**)], have been synthesized and characterized by elemental analysis, IR, XRD and single-crystal X-ray diffraction. X-ray structural analysis reveals that isostructral complexes **1–4** possess 3D structures with $4^6 6^4$ topology. Complexes **1** and **2** exhibit broad intraligand fluorescent emission bands. Complexes **3** and **4** not only display intraligand fluorescent emission bands, but also present Nd(III) characteristic emission in the near-IR region and sensitized luminescence of Dy(III) ions in the visible region, respectively. Variable-temperature magnetic susceptibility measurements of **2–4** have been studied over the temperature range of 4–300 K.

Keywords: Lanthanide; 5-sulfosalicylate; Topology; Luminescence; Magnetism

1. Introduction

The construction of coordination polymers has been a field of rapid growth not only for their intriguing architectures and topologies but also for their applications in areas of catalysis, sorption, separation, luminescence, magnetism, non-linear optical property, etc. [1–4]. Intense research has resulted in a large number of coordination polymers with novel structures and interesting properties [5–7]. Though the predictable coordination geometries of transition metals appear to be more attractive for design and tailor-making of coordination polymers, the lanthanide centers, with their high and variable coordination numbers and flexible coordination environment, are also beginning to garner the attention of chemists [8,9]. In particular, lanthanide ions may give amusing properties such as luminescence properties in both visible and near-IR regions, for example, the near-IR luminescence from Nd-containing systems have been regarded as the most popular infrared luminescence materials for application in laser systems [10]. It is well known that direct excitation of the $4f$–$4f$ transitions is difficult due to the low optical cross section of lanthanide ions arising from the forbidden nature of these transitions [11–13]. To enhance absorption, lanthanide ions are coordinated with organic ligands having broad and intense absorption bands in the UV-region. Otherwise, an assembly of metal ions and ligands in coordination polymers can be regarded as a programmed system in which the stereo and interactive information stored in the ligands is read by the metal ions through the algorithm defined by their coordination geometry [14]. Hence, the design or selection of a suitable ligand containing certain features, such as flexibility and versatile binding modes, is also crucial in the building of coordination polymers. The choice of 5-sulfosalicylic acid (H_3SSA) can be attributed to the following reasons: (a) it has three potential coordinating groups: –COOH, $–SO_3H$, and –OH in which the oxygen atoms can act as hard bases being strongly coordinated by Ln(III) ions behaved as hard acids, (b) it has a high structuring effect because its π-system and donor oxygen atoms take part in hydrogen bonding and aryl ring can act as a sensitizer for the lanthanide-centered luminescence by energy transfer from a ligand-centered

*Corresponding author. Fax: +86 431 85168624.
E-mail address: xjq@mail.jlu.edu.cn (J.-Q. Xu).

0022-4596/$ - see front matter © 2007 Elsevier Inc. All rights reserved.
doi:10.1016/j.jssc.2007.12.027

excited state (antenna effect) [15], (c) 5-sulfosalicylic acid has been found to have biological activity and its metal complexes exhibit anti-microbial activity stronger than that of the free ligand [16] and (d) it has an asymmetry geometry that may lead to compounds possessing acentric crystal structures, and only such compounds can act as candidates of second-order non-linear optical materials [17]. So far, most of the complexes with 5-sulfosalicylate ligands reported possess discrete [18–26], one- (1D) [26–34] or two-dimensional (2D) [32–41] structures, while only two transition metal- and one lanthanide-5-sulfosalicylate complexes having 3D structures have been reported [41–44]. In addition, many examples of the complexes containing 5-sulfosalicylate ligands in which a metal center is coordinated by one [25,33,38,42], two [27,29,34,35,41], three [35,41,42], four [35,37–39], and eight 5-sulfosalicylates [43] have been reported, but only one complex in which one metal atom is coordinated five 5-sulfosalicylates [44], is known. In this paper, we report the syntheses, structure characterizations, luminescence, and magnetism properties of four 3D lanthanide-5-sulfosalicylate coordination polymers with 5-connected $4^6 6^4$ topology—$Ln(SSA)(H_2O)_2$ [Ln = Ce(III) (**1**), Pr(III) (**2**), Nd(III) (**3**), and Dy(III) (**4**), H_3SSA = 5-sulfosalcycli acid]. A new coordination mode of SSA^{3-} is observed in these four complexes [26].

2. Experimental section

2.1. Material and methods

All chemicals purchased were of reagent grade and used without further purification. Elemental analyses (C, H) were performed on a Perkin-Elmer 240C elemental analyzer. The sulfur contents were established by the Schöniger combustion flask technique. IR spectra were measured on a Perkin-Elmer Spectrum One FT-IR spectrometer using KBr pellets. Powder XRD data of complexes **1–4** were collected on a Shimadzu XRD-6000 diffractometer with Cu-$K\alpha$ ($\lambda = 1.5418$ Å). The luminescence spectrum of complex **3** was performed at room temperature using a fluorescence spectrometer with an Ar ion laser (PL9000, BIO-RAD, UK) and the Ge detector worked at liquid nitrogen temperature. The visible luminescence properties of complexes **1–4** were measured on a Perkin-Elmer LS55 spectrometer. Magnetic measurements were obtained using an MPMS-XL5 magnetometer in the temperature range of 4–300 K. Diamagnetic corrections were made with Pascal's constants for all the constituent atoms [45].

2.2. Syntheses of $[Ln(SSA)(H_2O)_2]_n$ (1–4) [Ln = Ce(III) (1), Pr(III) (2), Nd(III) (3) and Dy(III) (4)

Complexes **1–4** were prepared under hydrothermal conditions. Lanthanide salts [$Ce(NO)_3 \cdot 6H_2O$ (0.22 g, 0.5 mmol) for **1**, $Pr(NO)_3 \cdot 6H_2O$ (0.22 g, 0.5 mmol) for **2**, $Nd(NO)_3 \cdot 6H_2O$ (0.22 g, 0.5 mmol) for **3,** and $Dy(NO)_3 \cdot 6H_2O$ (0.23 g, 0.5 mmol) for **4**], H_3SSA (0.13 g, 0.5 mmol), imidazole (0.056 g, 0.8 mmol), KOH (0.08 g, 1.5 mmol), and water (20 ml) were stirred for ca. 2 h, then the mixtures in a 25 ml Teflon-lined stainless steel vessel were heated under autogenous pressure at 160 °C for 72 h and finally cooled to room temperature. Colorless club-shaped crystals of **1** and **4**, pale-green club-shaped crystals of **2** and pale-violet club-shaped crystals of **3** were filtered, washed with distilled water and dried at ambient temperature. Yield: 0.058 g (33.6%, based on cerium) for **1**, 0.115 g (65.8%, based on praseodymium) for **2**, 0.126 g (72.4%, based on neodymium) for **3**, 0.052 g (27.8%, based on dysprosium) for **4**. Complexes **1–4** are insoluble in water as well as common organic solvents, and they are all stable in atmosphere. Anal. calcd. for $C_7H_7CeO_8S$ (391.31) **1**: C, 21.47; H, 1.79; S, 8.18%. Found: C, 21.35; H, 1.70; S, 8.26%. Anal. calcd. for $C_7H_7O_8PrS$ (392.10) **2**: C, 21.42; H, 1.79; S, 8.16%. Found: C, 20.96; H, 1.68; S, 8.32%. Anal. calcd. for $C_7H_7NdO_8S$ (395.43) **3**: C, 21.26; H, 1.78; S, 8.11%. Found: C, 20.98; H, 1.69; S, 8.03%. Anal. calcd. for $C_7H_7DyO_8S$ (413.69) **4**: C, 20.31; H, 1.69; S, 7.74%. Found: C, 19.83; H, 1.80; S, 7.66%.

IR (cm^{-1}) for **1**: 3552.89m, 3123.42m, 1606.23s, 1555.00s, 1505.41s, 1422.77s, 1376.80m, 1321.76m, 1257.27m, 1187.68s, 1161.66m, 1139.42s, 1088.20w, 1047.69m, 909.56w, 811.58w, 602.76s; for **2**: 3553.61m, 3125.44m, 1606.19s, 1555.06s, 1504.52s, 1422.81s, 1378.34m, 1322.20m, 1250.59m, 1190.75s, 1161.22s, 1139.28s, 1088.26w, 1048.61m, 909.84w, 811.83w, 602.47s; for **3**: 3565.14m, 3124.74m, 1606.50s, 1555.47s, 1504.62s, 1423.21s, 1379.58m, 1322.93m, 1257.71m, 1192.84s, 1161.49m, 1139.25s, 1088.58w, 1050.39m, 910.48w, 812.13w, 602.48s; for **4**: 3566.48m, 3126.09m, 1606.74s, 1556.17s, 1504.75s, 1423.54s, 1378.09s, 1322.40m, 1258.07m, 1191.82s, 1161.69m, 1140.26s, 1088.32w, 1048.24m, 909.99w, 812.03w, 602.90w.

2.3. X-ray crystallography

The crystal structures were determined by single-crystal X-ray diffraction experiment. The reflection data were collected on a Bruker-AXS Smart CCD diffractometer (Mo$K\alpha$, $\lambda = 0.71073$ Å) at room temperature with ω-scan mode. Empirical adsorption correction was applied to all data using SADABS program. The structures were solved by direct methods and refined by full-matrix least squares on F^2 using SHELXTL 97 software [46]. For complexes **1–4**, additional symmetry elements were detected when PLATON [47] software was applied to the final refinement results. However, the structure determinations based on the suggested *Pnma* space group were unsuccessful, leading to very poor convergence with high R_{sym} after integration and large anisotropic displacement parameters (for O atoms of sulfonate) were also present in this refinement. Additionally, though the flack parameters were equal approximately to 0.5 in the structures derived from $P2_12_12_1$ space group,

Table 1
The crystallographic data for complexes **1–4**

Complex	**1**	**2**	**3**	**4**
Empirical formula	$C_7H_7CeO_8S$	$C_7H_7O_8PrS$	$C_7H_7NdO_8S$	$C_7H_7DyO_8S$
Formula weight	391.31	392.10	395.43	413.69
Crystal system	Orthorhombic	Orthorhombic	Orthorhombic	Orthorhombic
Space group	$P2_12_12_1$	$P2_12_12_1$	$P2_12_12_1$	$P2_12_12_1$
a (Å)	7.0194(14)	7.0073(14)	6.9758(14)	6.9742(17)
b (Å)	9.5224(19)	9.4981(19)	9.4687(19)	9.477(2)
c (Å)	14.208(3)	14.216(3)	14.191(3)	14.174(4)
V (Å)	949.7(3)	946.2(3)	937.3(3)	936.8(4)
Z	4	4	4	4
$\rho_{calcd.}$ ($g\,cm^{-3}$)	2.737	2.753	2.802	2.933
Absorption coef. (mm^{-1})	5.044	5.402	5.794	8.231
θ range (deg)	3.24–27.47	3.24–27.43	3.25–27.44	2.59–28.48
Reflections collected	9265	9291	9230	6856
Unique reflections (R_{int})	2153 (0.0280)	2153 (0.0256)	2131 (0.0256)	2348 (0.0975)
Completeness (%)	99.6	99.8	99.8	99.1
Goodness-of-fit on F^2	1.096	0.908	0.929	0.984
Flack parameter	0.53(2)	0.50(2)	0.53(2)	0.57(4)
R indexes [$I>2\sigma(I)$][a]	$R_1 = 0.0203$, $wR_2 = 0.0403$	$R_1 = 0.0190$, $wR_2 = 0.0396$	$R_1 = 0.0195$, $wR_2 = 0.0403$	$R_1 = 0.0469$, $wR_2 = 0.0998$
R (all data)[a]	$R_1 = 0.0219$, $wR_2 = 0.0408$	$R_1 = 0.0202$, $wR_2 = 0.0400$	$R_1 = 0.0204$, $wR_2 = 0.0407$	$R_1 = 0.0689$, $wR_2 = 0.1088$

[a] $R_1 = \sum ||F_o| - |F_c|| / \sum |F_o|$; $wR = [\sum w(F_o^2 - F_c^2)_2 / \sum w(F_o^2)^2]^{1/2}$.

the values of the mean $|E^*E-1|$ (0.821, 0.803, 0.848, and 0.881 for **1–4**, respectively) being between 0.968 (centrosym) and 0.736 (non-centrosym) make sure the $P2_12_12_1$ space group is acceptable. This is the result of racemic twinning [48,49]. Non-hydrogen atoms were refined anisotropically. The hydrogen atoms were located from difference maps and refined with isotropic temperature factors in complexes **1–3**. For complex **4**, aromatic hydrogen atoms were placed in calculated positions and refined isostropically, while the hydrogen atoms of the water molecules were located in differences Fourier maps. Hydrogen atoms of the water molecules are refined with the restraints of O–H = 0.85(1) Å in complexes **1–4**. All calculations were carried out using SHELXTL 97 [46]. The crystallographic data and pertinent information are summarized in Table 1. The selected bond lengths are listed in Table 2.

Table 2
Selected bond lengths (Å) for **1–4**

1[a]			
Ce(1)–O(3)	2.391(2)	Ce(1)–O(8W)	2.511(4)
Ce(1)–O(2)	2.412(3)	Ce(1)–O(7W)	2.566(4)
Ce(1)–O(1)#1	2.413(2)	Ce(1)–O(4)#3	2.572(4)
Ce(1)–O(6)#2	2.480(4)	Ce(1)–O(5)#4	2.573(4)
2[b]			
Pr(1)–O(3)	2.376(2)	Pr(1)–O(8W)	2.504(3)
Pr(1)–O(2)	2.398(3)	Pr(1)–O(5)#4	2.544(4)
Pr(1)–O(1)#1	2.402(2)	Pr(1)–O(7W)	2.555(4)
Pr(1)–O(6)#3	2.463(4)	Pr(1)–O(4)#2	2.556(3)
3[c]			
Nd(1)–O(3)#1	2.373(2)	Nd(1)–O(8W)	2.489(4)
Nd(1)–O(2)#1	2.394(3)	Nd(1)–O(4)#4	2.515(4)
Nd(1)–O(1)	2.381(2)	Nd(1)–O(5)#3	2.517(4)
Nd(1)–O(6)#2	2.454(4)	Nd(1)–O(7W)	2.530(4)
4[d]			
Dy(1)–O(3)	2.381(6)	Dy(1)–O(4)#2	2.450(10)
Dy(1)–O(2)	2.387(7)	Dy(1)–O(8W)	2.484(8)
Dy(1)–O(1)#1	2.393(6)	Dy(1)–O(5)#3	2.532(10)
Dy(1)–O(6)	2.554(11)	Dy(1)–O(7W)	2.552(9)

[a] Symmetry codes for complex **1**: #1 $-x+2$, $y-1/2$, $-z+1/2$; #2 $x-1/2$, $-y+3/2$, $-z$; #3 x, $y-1$, z; #4 $x+1/2$, $-y+3/2$, $-z$.
[b] Symmetry codes for complex **2**: #1 $-x$, $y+1/2$, $-z+1/2$; #2 $x-1/2$, $-y+1/2$, $-z$; #3 $x+1/2$, $-y+1/2$, $-z$; #4 x, $y+1$, z.
[c] Symmetry codes for complex **3**: #1 $-x$, $y+1/2$, $-z+1/2$; #2 $-x-1/2$, $-y+2$, $z+1/2$; #3 $-x+1/2$, $-y+2$, $z+1/2$; #4 $-x$, $y-1/2$, $-z+1/2$.
[d] Symmetry codes for complex **4**: #1 $-x$, $y-1/2$, $-z+3/2$; #2 $x-1/2$, $-y+1/2$, $-z+1$; #3 $x+1/2$, $-y+1/2$, $-z+1$.

3. Results and discussion

3.1. Syntheses

The hydrothermal method has been proven to be very effective for the syntheses of coordination polymers. It is well known that small changes in one or more of hydrothermal parameters, such as temperature, reaction time, pH value, and molar ratio of the reactants, etc., sometimes may exert profound influence on final reaction products.

Complexes **1–4** were successfully prepared with good yields through hydrothermal reaction at 160 °C for 72 h. Under other reaction condition being unchanged, crystal products of complexes **1–4** with lower yields were obtained when reaction temperature is at 170 °C, while at 150 °C powder products were got, which have been proved to be complexes **1–4**, respectively, by their IR spectra and XRD (Fig. S1).

It should be mentioned that although the synthetic procedures of complexes **1–4** were similar to [Ln(SSA)$(H_2O)_2]_n \cdot nH_2O$ gained at reaction temperature 120 °C [39], the structures of the former being 3D frameworks are fully different from 2D sheet of the latter. This difference probably results from different reaction temperatures.

3.2. Crystal structure of complexes *1–4*

The structure determination of complexes Ln(SSA)$(H_2O)_2$ [Ln = Ce(**1**), Pr(**2**), Nd(**3**), and Dy(**4**)] reveals that they are isostructral 3D frameworks and crystallize in orthorhombic system, $P2_12_12_1$ space group. Each Ln(III) is surrounded by an O_8 environment formed by two coordinated water molecules and five symmetry-related SSA^{3-} ligands in which three different SSA^{3-} ligands each provide one sulfonate group oxygen atom (O4, O5 and O6), the fourth SSA^{3-} ligand gives one carboxylate atom (O2) and one hydroxyl oxygen atom (O3) and the fifth one provides a carboxylate oxygen atom (O1) to Ln(III) atom, respectively (Fig. 1a). The Ln–O bond distances are in the range of 2.391(2)–2.573(4) Å in **1** (Ln = Ce), 2.377(3)–2.556(5) Å in **2** (Ln = Nd), 2.373(3)–2.525(4) Å in **3** (Ln = Nd), and 2.381(11)–2.554(9) Å in **4** (Ln = Dy), showing gradual decrease of Ln–O distances from Ce(III) **1** to Nd(III) **3** except Dy(III) **4**, being consistent with the radius contraction from Ce to Nd [50,51]. A new μ_5 coordination mode of SSA^{3-} ligand was found in complexes **1–4** (Fig. 1b) [26]. Three oxygen atoms (O4, O5 and O6) of the sulfonate group each links an Ln atom, an oxygen atom (O1) of the carboxylate group connects an Ln atom, while another oxygen atom (O2) of the carboxylate group and oxygen atom (O3) of deprotonated hydroxyl group together chelate an Ln atom for a SSA^{3-} ligand. As shown in Fig. 2, two adjacent SSA^{3-} ligands

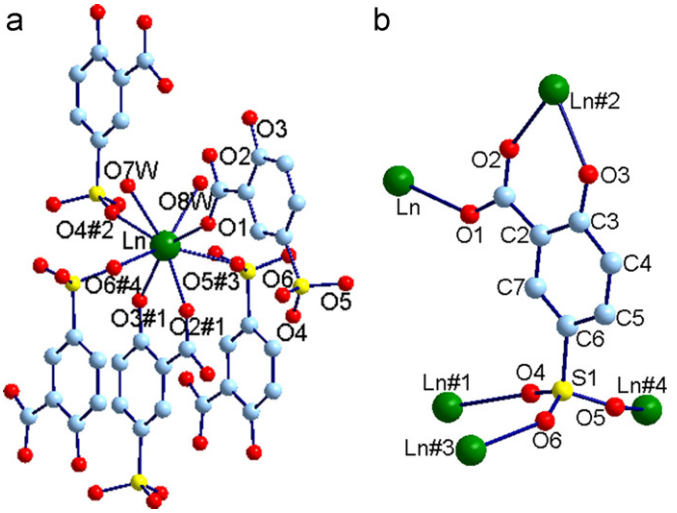

Fig. 1. (a) Coordination environment of Ln(III) in complexes **1–4**. Colors for coding atoms: Ln: green; C: pale blue; O: red; S: yellow. (b) Coordination mode of SSA^{3-} ligand. Symmetry codes: #1, $-x$, $0.5+y$, $0.5-z$; #2, $-x$, $-0.5+y$, $0.5-z$; #3, $-0.5-x$, $2-y$, $-0.5+z$; #4, $0.5-x$, $2-y$, $-0.5+z$.

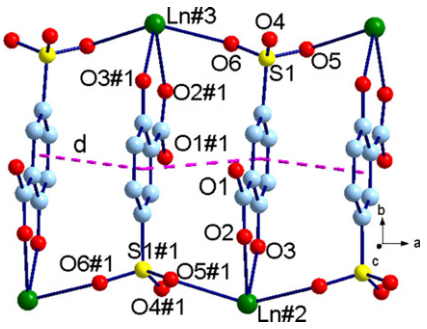

Fig. 2. The infinite double chain in complexes **1–4** containing head-to-tail arrangement. Symmetry codes: #1, $-0.5+x$, $1.5-y$, $-z$; #2, $-x$, $-0.5+y$, $0.5-z$; #3, $-0.5-x$, $2-y$, $-0.5+z$.

link two Ln(III) ions to O2, O3, O5 and O6 atoms into a 16-membered ring $Nd_2S_2C_8O_4$ in head-to-tail packing, which connect each other to form an infinite double-chain running along *a*-axis. This arrangement is stabilized by significant π–π interactions: the aromatic phenyl of SSA^{3-} ligands are stacked almost parallel and the dihedral angle (θ) between adjacent ones is 2.091°, and the centroid-to-centroid distance (*d*) between adjacent aromatic rings is 3.713 Å being within the range required for π–π interactions [52]. The resulting chains are, again, aggregated into a corrugated layer to O4 of the sulfonate group and its symmetric partners (Fig. 3a). The neighboring corrugated layers are further connected by O1 of carboxylate group and its symmetrically relevant atoms projecting outwards on opposite side of the layers to give rise to a 3D framework in which there are 1D channels running along *a*-axis (Fig. 3b), while along *b*- and *c*-axis there exist no channels. The 1D channels consist of 12-membered rings formed from two Ln, four O (two O1, one O2, and one O4), one S and five C (two C1, C2, C6 and C7 each one) atoms, and cross-section size of the channels is about 7.186×5.202 Å^2. The strong H-bonds involving the two water oxygen atoms (O7W and O8W) as donors and O2, O3 and O5 as accepters stabilize the 3D framework. The corresponding parameters of H-bonds are summarized in Table 3.

Better insight into the nature of 3D framework structures in the complexes can be achieved by the application of topological approach. In complexes **1–4**, each Ln(III) center being connected with five SSA^{3-} is considered as a 5-connected inorganic node (Fig. 4a) and each SSA^{3-} coordinating with five metal centers is regard as 5-connected organic node (Fig. 4b). The inorganic nodes and the organic nodes interlinked into inorganic–organic 3D topology network (Fig. 4c) with a Schläfli symbol 4^66^4 which denotes that six 4-gons and four 6-gons are adopted around each 5-connected node (the topological symbol refers to the "shortest circuits" formed around the 5-connected nodes). Although a large number of examples of 3-, 4-, and 6-connected networks have been reported [53], the ones with 5-connected networks are relatively rare [54], to the best of our knowledge, there are only a few

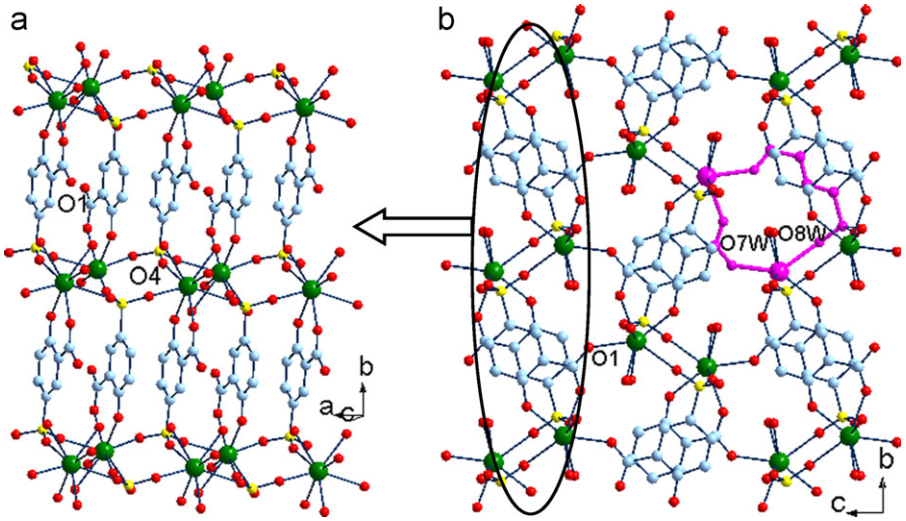

Fig. 3. (a) A view of corrugated layer. (b) A view of 3D framework interlinked by 2D corrugated layers (ellipse part). Highlighting shows the 1D channel.

Table 3
Geometrical parameters of hydrogen bonds (Å) in complex **3**

D–H···A	*d*(D–H)	*d*(H···A)	*d*(D···A)	<DHA
O8W–H8WA···O3	0.845	2.418	2.867	113.92
O7W–H7WA···O3	0.849	2.204	3.021	161.74
O8W–H8WB···O2	0.841	2.130	2.872	146.85
O7W–H7WB···O2	0.844	2.306	2.914	129.22
O7W–H7WB···O5	0.844	2.522	3.208	139.08

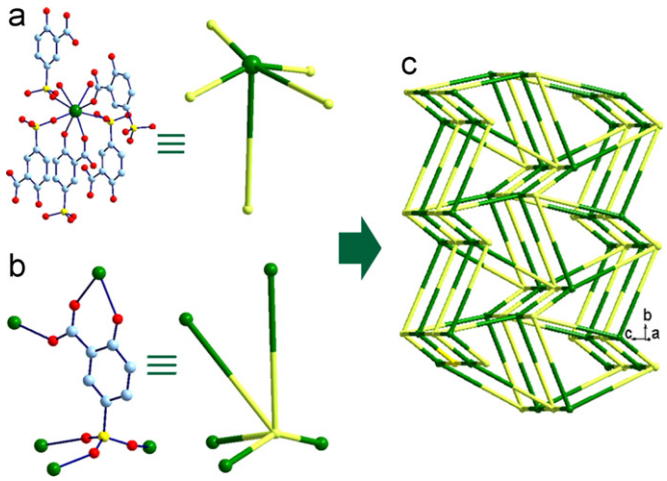

Fig. 4. (a) A 5-connected inorganic node containing one metal center with five SSA^{3-}. (b) A 5-connected organic node containing one SSA^{3-} with five mental centers. (c) Schematic representation of the 3D $4^6 6^4$ topology network.

reported examples containing 5-connected metal centers with $4^6 6^4$ topology [55–57].

Although complexes **1–4** and previously reported $[Ln(SSA)(H_2O)_2]_n \cdot nH_2O$ [39] have similar empirical formulae, their structures are distinctly different. Firstly, each Ln(III) in complexes **1–4** connects five SSA^{3-} ligands, while in the latter each Ln(III) links four SSA^{3-} ligands. Secondly, each SSA^{3-} ligand coordinate to five Ln(III) centers in complexes **1–4** and thus can be regard as a μ_5 connector, while in the latter each SSA^{3-} ligand coordinates to four Ln(III) centers and thus can act as a μ_4 connector. All of these lead to the formation of more higher dimensional (3D) frameworks of complexes **1–4** but not 2D sheets of the latter.

3.3. XRD analyses

We examined the structural homogeneity of bulk powder samples of **1–4** through comparison of experimental and simulated powder XRD patterns. The peak positions of the experimental patterns are in agreement with that of the simulated ones generated from single-crystal X-ray diffraction data (Fig. 5), which indicates the phase purities of complexes **1–4**. The intensities of the experimental XRD patterns are a little weak, due to the preferred orientation of the powder samples and the instrumental limitations.

3.4. Luminescence properties

It is well known that ligand sensitized lanthanide luminescence occurs when an organic ligand, which is coordinated to the metal ion, collects UV excitation energy and channels it in a radiationless process through the triplet state to the resonant level of the lanthanide ion which emits its characteristic luminescence. The solid-state luminescent properties of complexes **1–4** were investigated at room temperature. The emission spectra of H_3SSA ligand and **1–3** are shown in Fig. 6. The emission band at $\lambda_{max} = 389$ nm when excited at 335 nm for the free H_3SSA ligand is attributable to the $\pi^* \rightarrow n$ or $\pi^* \rightarrow \pi$ transitions. The emission spectra of complexes **1–3** show broad emissions at about $\lambda_{max} = 389$ nm when excited at 335 nm

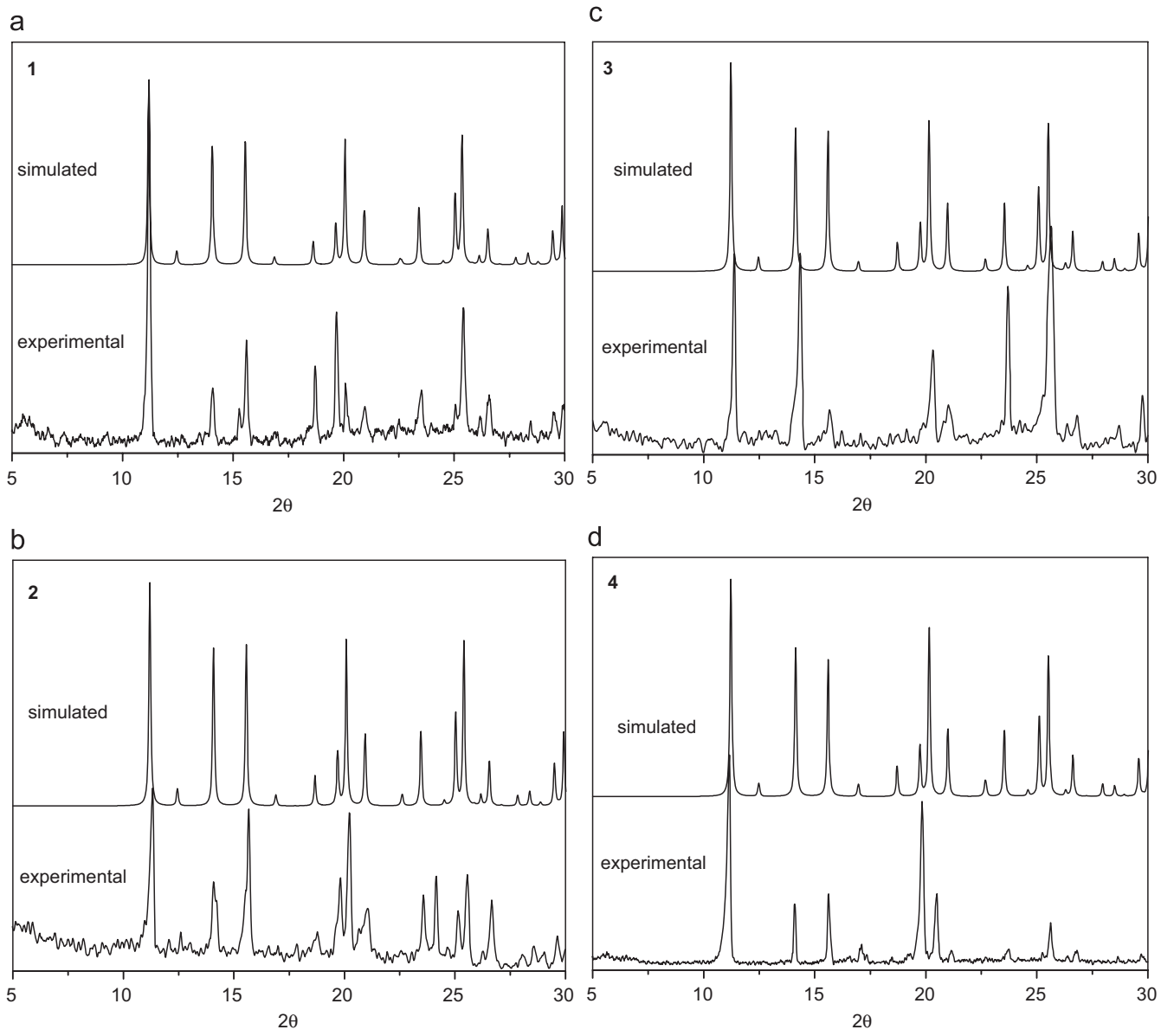

Fig. 5. The experimental and simulated XRD patterns for complexes **1** (a), **2** (b), **3** (c), and **4** (d).

which would be assigned to the emission of intraligand fluorescent emission. Moreover, complex **3** shows the characteristic emission bands when excited at 488 nm for the Nd(III) ion (Fig. 7) in the near-IR region: the three bands at $\lambda = 905$, 1055 and 1328 nm are attribute to the *f–f* transition $^4F_{3/2} \rightarrow {}^4I_{9/2}$, $^4F_{3/2} \rightarrow {}^4I_{11/2}$ and $^4F_{3/2} \rightarrow {}^4I_{13/2}$, respectively. The emission spectrum of **4** at room temperature in solid state excited at 355 nm is shown in Fig. 8. The main broad and strong band in the 335–440 nm at $\lambda_{max} = 382$ nm are due to the $\pi^* \rightarrow$n or $\pi^* \rightarrow \pi$ transition of organic ligand. The smaller emissions at 484 and 577 nm correspond to the typical characteristic emission $^4F_{9/2} \rightarrow {}^6H_{15/2}$ and $^4F_{9/2} \rightarrow {}^6H_{13/2}$ of Dy(III) ions [58]. The relatively weak emission intensity for Dy(III) ions implies that the efficiency of energy-transfer from ligand to metal is low. No near-IR fluorescence emission spectrum was observed for **2**, though the sensitization of the near-IR luminescence of Pr(III) ions has been achieved by suitable ligands [59,60]. This indicates that the SSA cannot sensitize the near-IR luminescence of Pr(III) ions.

3.5. Magnetism properties

We investigated the magnetic properties of complexes **2** at 1 T, and **3** and **4** at 0.1 T within the temperature range of 4–300 K.

For **2** (Pr), the $\chi_M T$ vs. T and χ_M^{-1} vs. T curves are shown in Fig. 9. The observed $\chi_M T$ of the Pr(III) ion at room temperature is equal to 1.40 $cm^3\,mol^{-1}\,K$, which leads to an effective magnetic moment μ_{eff} of $3.45\mu_B$ being slightly lower than the theoretical value of $3.58\mu_B$ for a free Pr(III)

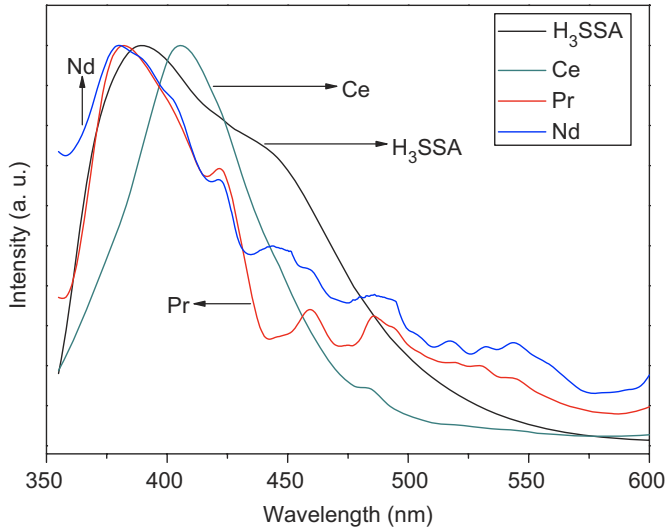

Fig. 6. Normalized solid-state emission spectra ($\lambda_{ex} = 335$ nm) of H_3SSA ligand and complexes **1–3**.

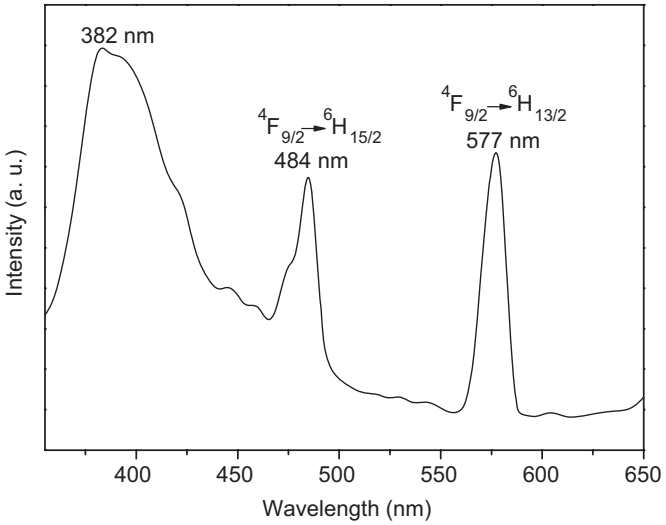

Fig. 8. Solid-state emission spectrum ($\lambda_{ex} = 335$ nm) of **4**.

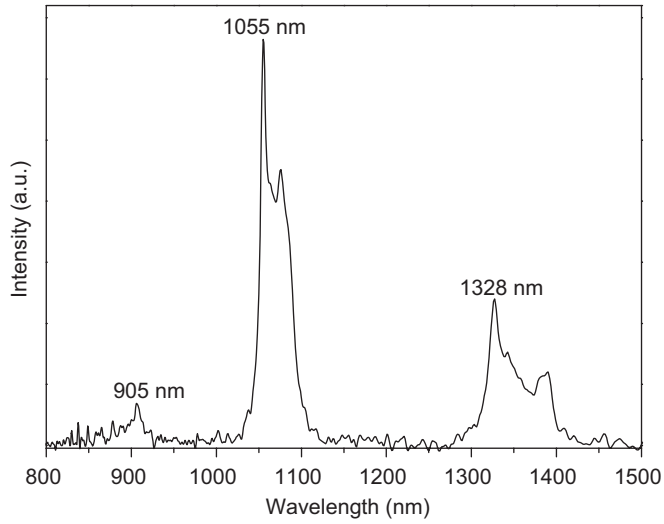

Fig. 7. Solid-state emission spectrum of **3** in the near-IR region.

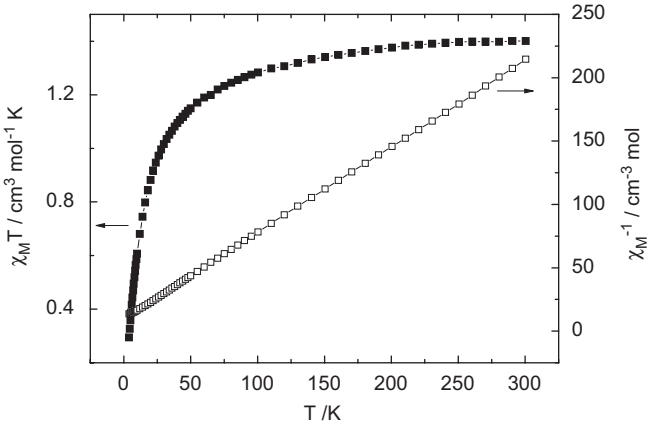

Fig. 9. Plots of $\chi_M T$ and χ_M^{-1} vs. T for **2**.

ion ground state ($^3H_4$) with two localized unpaired *f*-electrons. Upon temperature lowering, the $\chi_M T$ decreases gradually to a value of 0.29 $cm^3\,mol^{-1}\,K$ at 4 K, with an effective magnetic moment μ_{eff} of $1.53\mu_B$. The plot of χ_M^{-1} vs. T over the whole temperature range of 4–300 K obeys the Curie–Weiss law $\chi_M = C/(T-\theta)$, with Curie constant $C = 1.70\,cm^3\,K\,mol^{-1}$ and Weiss constant $\theta = -17.99$ K. All of these results indicate that there is a weak anti-ferromagnetic interaction between the Pr(III) ions in **2**.

The magnetic characteristic of complex **3** is similar to that of complex **2**. As can be seen from Fig. 10, the observed $\chi_M T$ of the Nd(III) ion at room temperature is 1.61 $cm^3\,mol^{-1}\,K$, which gives an effective magnetic moment μ_{eff} of $3.59\mu_B$ being close to the expected value of $3.62\mu_B$ for the free Nd(III) ion in the $^4I_{9/2}$ ground state. When dropping in temperature, the $\chi_M T$ gradually decreases to a value of 0.79 $cm^3\,mol^{-1}\,K$ at 4 K, with an effective magnetic moment μ_{eff} of $2.52\mu_B$. The plot of χ_M^{-1} vs. T over the whole temperature range of 4–300 K can be fit to the Curie–Weiss expression $\chi_M = C/(T-\theta)$, with Curie constant $C = 0.97\,cm^3\,K\,mol^{-1}$ and Weiss constant $\theta = -1.02$ K. Such behavior can be referred to the presence of a weak anti-ferromagnetic interaction between the Nd(III) ions.

For **4** (Dy), the observed $\chi_M T$ of the Dy(III) ion at room temperature (Fig. 11) is 15.20 $cm^3\,mol^{-1}\,K$, which gives an effective magnetic moment μ_{eff} of $11.03\mu_B$ being slightly higher than the theoretical value of $10.65\mu_B$ for the free Dy(III) ion. On lowering the temperature, the $\chi_M T$ increases gradually to 16.32 $cm^3\,mol^{-1}\,K$ at 100 K and keeps on this value till 70 K, then rapidly decreases down to 4 K where its value is 13.06 $cm^3\,mol^{-1}\,K$. The plot of χ_M^{-1} vs. T follows the Curie–Weiss law in the temperature range of 70–300 K with Curie constant $C = 14.88\,cm^3\,K\,mol^{-1}$ and Weiss constant $\theta = 6.43$ K.

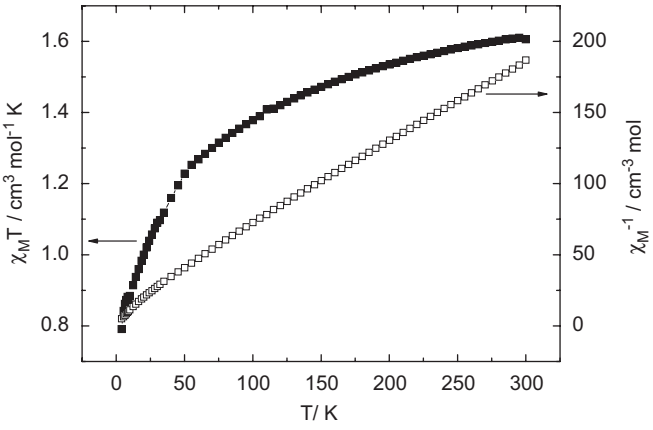

Fig. 10. Plots of $\chi_M T$ and χ_M^{-1} vs. T for **3**.

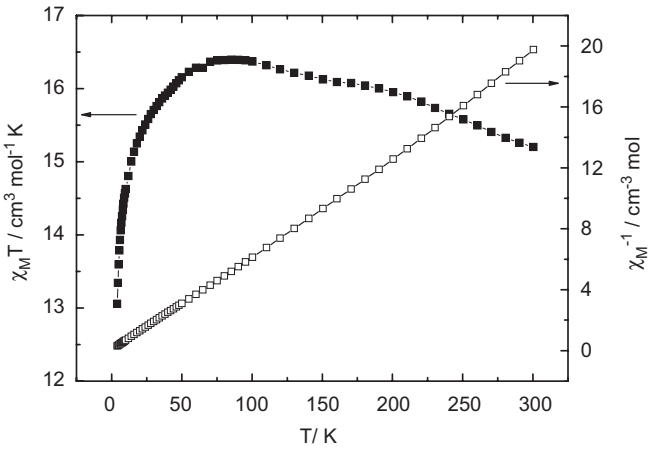

Fig. 11. Plots of $\chi_M T$ and χ_M^{-1} vs. T for **4**.

4. Conclusion

In summary, four new lanthanide complexes constructed by 5-sulfosalicylic acid have been synthesized by hydrothermal reactions and structurally characterized. Complexes **1–4** possess 3D framework structures with relatively rare 5-connected $4^6 6^4$ topology. The structures verify that high and variable coordination numbers and flexible coordination environment of lanthanide ions suit the formation of frameworks with highly connected nodes. The solid-state luminescent spectra demonstrate that complexes **1–4** exhibit strong intraligand fluorescent emission bands in the visible region, moreover, complexes **3** and **4** show Nd(III) characteristic emission in the near-IR region and sensitized luminescence of Dy(III) in the visible region, respectively. Variable-temperature magnetic susceptibility measurements of **2** and **3** indicate that there exist anti-ferromagnetic interactions between magnetic centers. Ferromagnetic interactions can be observed in complex **4**.

Acknowledgment

This work was supported by the National Natural Science Foundation of China (Grant nos. 20571032 and 20333070).

Appendix A. Supporting information available

X-ray crystallographic files of complexes **1–4** in **CIF** format, CCDC reference numbers: 652,403, 652,404, 652,405, and 652,406 for complexes **1–4**, respectively. Supplementary crystallographic data associated with this paper can be obtained free of charge from The Cambridge Crystallographic Data Centre via http://www.ccdc.cam.ac.uk/data_request/cif.

Supplementary data associated with this article can be found in the online version at doi:10.1016/j.jssc.2007.12.027.

References

[1] B. Moulton, M.J. Zaworotko, Chem. Rev. 101 (2001) 1629.
[2] N.L. Rosi, J. Echert, M. Eddaoudi, D.T. Vodal, J. Kim, M. O'Keeffe, O.M. Yaggi, Science 300 (2003) 1127.
[3] O.M. Yaghi, H. Li, C. Davis, D. Richardson, T.L. Groy, Acc. Chem. Res. 31 (1998) 474.
[4] C.N. Rao, S. Natarajan, R. Vaidhyanathan, Angew. Chem. Int. Ed. 43 (2004) 1466.
[5] J.P. Zhang, Y.Y. Lin, X.C. Huang, X.M. Chen, J. Am. Chem. Soc. 127 (2005) 5495.
[6] K. Nakabayashi, M. Kawaano, M. Yoshizawa, S.I. Ohkoshi, M. Fujita, J. Am. Chem. Soc. 126 (2004) 16694.
[7] B. Zhao, P. Cheng, X.Y. Chen, C. Cheng, W. Shi, D.Z. Liao, S.P. Yan, Z.H. Jiang, J. Am. Chem. Soc. 126 (2004) 3012.
[8] J.Y. Kim, A.J. Norquist, D. O'Hare, Chem. Mater. 15 (2003) 1970.
[9] G.A. Lawrance, Chem. Rev. 86 (1986) 17.
[10] A. Rogalski, K. Chizanowski, Opto-Electron. Rev. 10 (2002) 111.
[11] Z. Hnatejko, A. Klonkowski, S. Lis, K. Czarnobaj, M. Pietraszkiewicz, M. Elbanowski, Mol. Cryst. Liq. Cryst. 354 (2000) 795.
[12] M. Kawa, J.M. Frechet, J. Chem. Mater. 10 (1998) 286.
[13] C. Piguet, J.C.G. Bunzli, G. Bernadellia, G. Hopfgartner, A.F. Williams, J. Am. Chem. Soc. 115 (1993) 8197.
[14] E. Antic-Fidancev, F. Serpaggi, G. Férey, J. Alloys Compds. 340 (2002) 88.
[15] R.E. Whan, G.A. Crosby, J. Mol. Spectrosc. 8 (1962) 315.
[16] P.V. Khadikar, S. Joshi, S.G. Kashkhedikar, B.D. Heda, Indian J. Pharm. Sci. 46 (1984) 209.
[17] K. Sénéchal, L. Toupet, I. Ledoux, J. Zyss, H.L. Bozec, O. Maury, Chem. Commun. (2004) 2180.
[18] S.R. Fan, L.G. Zhu, Acta Crystallogr. E 61 (2005) m2480.
[19] S.R. Fan, L.G. Zhu, H.P. Xiao, S.W. Ng, Acta Crystallogr. E 61 (2005) m377.
[20] B. Liu, Z.J. Wang, S.P. Huang, B.S. Yang, Acta Crystallogr. E 62 (2006) m608.
[21] J.F. Li, Y.J. Zhao, X.H. Li, M.L. Hu, Acta Crystallogr. E 60 (2004) m1210.
[22] S.R. Fan, G.Q. Cai, L.G. Zhu, H.P. Xiao, Acta Crystallogr. C 61 (2005) m177.
[23] S.R. Rong, L.G. Zhu, China J. Chem. 23 (2005) 1292.
[24] S.R. Fan, H.P. Xiao, L.G. Zhu, Acta Crystallogr. E 62 (2006) m18.
[25] W.X. Ma, B.H. Qian, J. Gao, X.Y. Xu, L.D. Lu, X.J. Yang, X. Wang, H.B. Song, China J. Inorg. Chem. 21 (2005) 612.
[26] J.F. Song, Y. Chen, Z.G. Li, R.S. Zhou, X.Y. Xu, J.Q. Xu, T.G. Wang, Polyhedron (2007) 4397.
[27] Z.F. Chen, S.M. Shi, R.X. Hu, M. Zhang, H. Liang, Z.Y. Zhou, China J. Chem. 21 (2003) 1059.
[28] E. Hecht, Acta Crystallogr. E 60 (2004) m1286.
[29] W.G. Wang, J. Zhang, L.J. Song, J.F. Ju, Inorg. Chem. Commun. 7 (2004) 858.
[30] S.R. Fan, L.G. Zhu, Acta Crystallogr. E 61 (2005) m2080.

[31] S.R. Fan, L.G. Zhu, H.P. Xiao, Acta Crystallogr. E 61 (2005) m804.
[32] F.F. Li, J.F. Ma, S.Y. Song, J. Yang, Cryst. Growth Des. 1 (2006) 209.
[33] S.R. Fan, L.G. Zhu, Inorg. Chem. 45 (2006) 7935.
[34] Z.D. Lu, L.L. Wen, Z.P. Ni, Y.Z. Li, H.Z. Zhu, Q.J. Meng, Cryst. Growth Des. 7 (2007) 268.
[35] H.Y. Sun, C.H. Huang, X.L. Jin, G.X. Xu, Polyhedron 14 (1995) 1201.
[36] S.R. Fan, L.G. Zhu, Acta Crystallogr. E 61 (2005) m174.
[37] P. Starynowicz, J. Alloys Compds. 305 (2000) 117.
[38] J.F. Ma, J. Yang, L. Li, G.L. Zheng, J.F. Liu, Inorg. Chem. Commun. 6 (2003) 581.
[39] Z.D. Lu, L.L. Wen, J. Yao, Z.Z. Zhu, Q.J. Meng, Cryst. Eng. Commun. (2006) 847.
[40] M.C. Hu, C.Y. Geng, S.N. Li, Y.P. Du, Y.C. Jiang, Z.H. Liu, J. Organomet. Chem. 690 (2005) 3118.
[41] J.F. Ma, J. Yang, S.L. Li, S.Y. Song, H.J. Zhang, H.S. Wang, K.Y. Yang, Cryst. Growth Des. 5 (2005) 807.
[42] A. Marzotto, D.A. Clemente, T. Gerola, G. Valle, Polyhedron 20 (2001) 1079.
[43] M.C. Hu, C.Y. Geng, S.N. Li, Y.P. Du, Y.C. Jiang, Z.H. Liu, J. Organomet. Chem. 690 (2005) 3118.
[44] X.Q. Wang, J. Zhang, Z.J. Li, Y.H. Wen, J.K. Cheng, Y.G. Yao, Acta Crystallogr. C 60 (2004) m657.
[45] E.A. Boudreaux, L.N. Mulay, Theory and Applications of Molecular Paramagnetism, Wiley, New York, 1976, p. 494.
[46] G.M. Sheldrick, SHELXS 97, Program for Crystal Structure Refinement, University of Göttingen, Göttingen, Germany, 1998.
[47] A.L. Spek, PLATON, Molecular Geometry Program, University of Utrecht, The Netherlands, 1999.
[48] A. Krief, T. Ollevier, D. Swinnen, B. Norberg, G. Baudoux, G. Evrard, Acta Crystallogr. C 54 (1998) 392.
[49] W. Li, H.P. Jia, Z.F. Ju, J. Zhang, Cryst. Growth Des. 4 (2006) 2136.
[50] U. Abram, D.B. Dell'Amico, F. Calderazzo, C.D. Porta, U. Englert, F. Marchetti, A. Merigo, Chem. Commun. (1999) 2053.
[51] L. Pan, X. Huang, J. Li, Y. Wu, N. Zheng, Angew. Chem., Int. Ed. 39 (2000) 527.
[52] C. Janiak, J. Chem. Soc. Dalton Trans. (2000) 3885.
[53] N.W. Ockwig, O.D. Friedrichs, M. O'Keeffe, O.M. Yaghi, Acc. Chem. Res. 8 (2005) 176.
[54] M. O'Keeffe, M. Eddaoudi, H. Li, T. Reineke, O.M. Yaghi, J. Solid State Chem. 152 (2000) 3.
[55] D.L. Long, A.J. Blake, N.R. Champness, C. Wilson, M. Schröder, J. Am. Chem. Soc. 123 (2001) 3401.
[56] L. Pan, N. Ching, X.Y. Huang, J. Li, Chem. Commun. (2001) 1064.
[57] H.L. Sun, B.Q. Ma, S. Gao, S.R. Batten, Cryst. Growth Des. 4 (2006) 209.
[58] C. Tedeschi, J. Azema, H. Gornitzka, P. Tisnes, C. Picard, Dalton Trans. (2003) 1738.
[59] S. Quici, M. Cavazzini, G. Marzanni, G. Accorsi, N. Armaroli, B. Ventura, F. Barigelletti, Inorg. Chem. 44 (2005) 529.
[60] G.M. Davies, R.J. Aarons, G.R. Motson, J.C. Jeffery, H. Adams, S. Faulkner, M.D. Ward, Dalton Trans. (2004) 1136.